

# TRANSLUNAR LOGISTICS WITH LOW-ENERGY TRANSFERS

Nick Gollins\*, Yuri Shimane<sup>†</sup>, and Koki Ho<sup>‡</sup>

Low-energy lunar transfers (LETs) utilize three-body mechanics with fourth-body (solar) perturbations to provide an alternative to direct lunar transfers. The offer of reduced lunar orbit insertion cost in exchange for longer time-of-flight and potentially higher transfer insertion cost presents an interesting trade-off when planning the logistics of multi-mission lunar exploration campaigns. This is particularly true for logistics featuring spacecraft with a variety of launch vehicles and propellant types, as the logistics of each spacecraft are impacted by the costs and benefits of LETs differently. This paper presents a translunar logistics model featuring LETs, discusses the trade-offs versus direct transfers through some case studies, and highlights the scenarios in which LETs prove most useful.

## INTRODUCTION

Space logistics is an emerging field that exists at the intersection of space systems engineering, mission analysis, and operations research. Logistics was considered for lunar base architecture studies as early as the Apollo era and the decades that followed,<sup>1</sup> although operations research practices were not introduced until studies of ISS-supporting architectures were made.<sup>2,3</sup> The discipline has the overarching objective of finding efficient architectures for complex space missions or multi-mission campaigns. More recently, the expansion of the field has been driven by increasing capabilities in space, allowing for more complex architectures that require efficient design and operations. Logistics practices have since been applied to cislunar and interplanetary exploration,<sup>4-9</sup> on-orbit servicing,<sup>10,11</sup> debris removal,<sup>12</sup> and logistics infrastructure and vehicle system design.<sup>13-16</sup>

Commodity flow linear programming models find the optimal flow of commodities through a network that satisfies a set of supply and demand constraints. By adapting them to space exploration missions, they give a method by which to quickly evaluate the effectiveness of mission architectures by optimizing for minimum total launch mass. Additionally, optimal launch schedules for exploration campaigns can be found by wrapping the linear program model with a metaheuristic optimization algorithm.<sup>17,18</sup>

Most previous works on lunar logistics modeling thus far have considered only high-thrust, direct lunar transfers. Jagannatha *et al* studied combinations of low-thrust and low-energy lunar transfer trajectories,<sup>19</sup> and implemented low-thrust trajectories in an event-driven network optimization.<sup>20</sup> This method does not, however, enable multiple logistics vehicles to travel at the same time.

---

\*PhD Candidate, Daniel Guggenheim School of Aerospace Engineering, Georgia Institute of Technology, Atlanta, GA 30332.

<sup>†</sup>PhD Candidate, Daniel Guggenheim School of Aerospace Engineering, Georgia Institute of Technology, Atlanta, GA 30332.

<sup>‡</sup>Dutton-Duoffe Professor (Associate Professor), Daniel Guggenheim School of Aerospace Engineering, Georgia Institute of Technology, Atlanta, GA 30332.

To the best of the author’s knowledge, low-energy lunar transfers have not previously been implemented in a time-expanded logistics model. Low energy transfers provide interesting flexibility to campaign scheduling: a slow but more efficient transfer may be preferable to a direct one if the schedule and launch capability allows.<sup>21</sup> The following paper, therefore, aims to build on previous logistics models by implementing the choice of transfer type in order to find more efficient campaign scheduling solutions.

First, this paper will discuss the generation and selection of the considered low-energy transfers. Then, the logistics model formulation and exploration campaign scheduling method will be reviewed, detailing the necessary changes to the model in order to account for LETs. Finally, the trade-offs introduced by the LETs will be analyzed through a number of case studies, and the situations in which LETs can improve an exploration campaign will be discussed.

## METHOD

The overarching method of the exploration campaign scheduling algorithm is described in detail in previous work.<sup>18</sup> To summarize, the method works by using a genetic algorithm to find optimal supply/demand times for a series of payloads. The selected supply/demand times are used, in addition to a set of spacecraft system definitions, to construct a commodity flow linear program. The supplies/demands are attached to “nodes”, representing locations such as the Earth and the Moon. Commodities flow through the network along “arcs”. Each arc has a  $\Delta V$  and a time-of-flight (TOF) associated with it. In a static network, only the nodes and the arcs representing their spacial separation are considered. A network becomes “time-expanded” by repeating the static network across many discrete time steps, with “holdover” arcs connecting a location to its future counterpart. So every second discrete time step completes the repetitive period of the model. A mixed-integer linear program is used to find the flow that results in a minimized launch mass, subject to certain constraints.

The genetic algorithm seeks the schedule that produces the model which, when solved by the mixed-integer linear program (MILP) optimizer, has the lowest-cost (minimum total launch mass) commodity flow, given the set of programmatic requirements and vehicle definitions. Updates to the methods and logistics model made to facilitate the introduction of LETs will be described here.

### Trajectory Generation and Selection

A variety of low-energy lunar transfers were pre-computed by leveraging a grid-based back-propagation technique to obtain candidate weak-stability boundary transfers (WSBTs) in the Earth-Moon circular restricted three-body problem.<sup>22</sup> Candidate WSBTs designed to transfer the spacecraft into a near-polar low lunar orbit (LLO) with an inclination of  $90 \pm 5^\circ$  and an altitude of 100 km were further pruned by back-propagating from perilune using the Earth-Moon-Sun bi-circular restricted four-body problem (BCR4BP), with another grid search based on the angular position of the Sun with respect to the Earth-Moon line. The BCR4BP employed in this work assumed a coplanar Earth-Moon and Sun-Earth planes.

The dynamics model used is periodic with the Sun-Earth-Moon synodic period  $\approx 29.53$  days. Therefore, it is useful to express time in terms of the Sun angle  $\theta_s \in [0^\circ, 360^\circ]$ , defined to be positive counter clock-wise from the Earth-Moon line to the Earth-Moon barycenter-Sun line, illustrated in Figure 1. Note that in the Earth-Moon rotating plane, since the lunar sidereal period is shorter at  $\approx 27.3$  days, the Sun appears to rotate clockwise about the Earth-Moon barycenter, i.e.  $\dot{\theta}_s \approx$

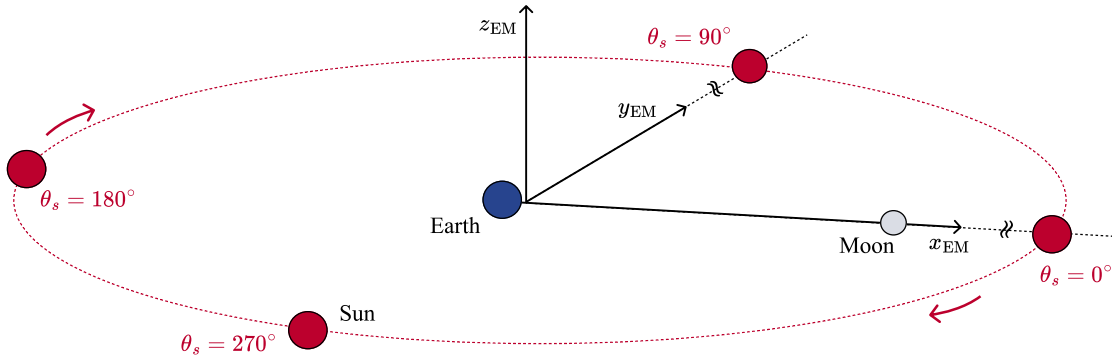


**Figure 1:** Rotation of the Sun about the Earth-Moon barycenter in the Earth-Moon rotating frame throughout the Earth-Moon-Sun synodic period.

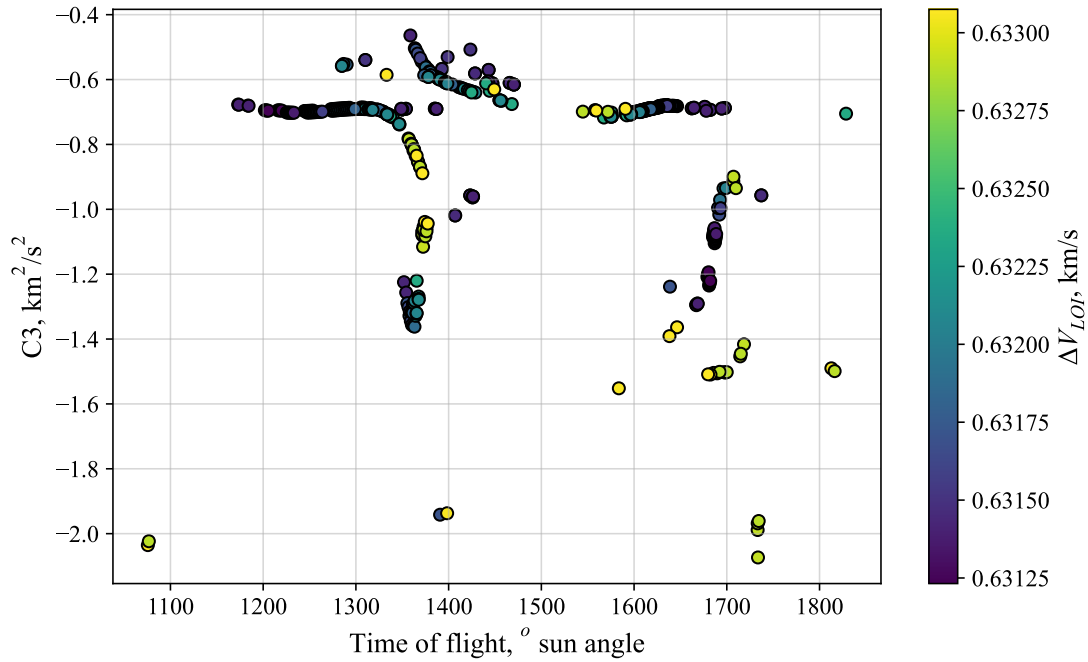
$-0.9253$  rad/s. Then, neglecting the lunar obliquity, the local time at  $0^\circ$  longitude on the Moon can be expressed as  $\theta_s = 270^\circ$  at Sun rise,  $\theta_s = 180^\circ$  at noon,  $\theta_s = 90^\circ$  at Sun set, and  $\theta_s = 0^\circ$  at midnight.

The key characteristics of the set of trajectories generated are shown in Figure 2. Lunar orbit insertion (LOI)  $\Delta V$  does not vary significantly between transfers, but the transfer  $C_3$  varies significantly. This translates to a variation in lunar transfer injection (LTI)  $\Delta V$ . There is a relatively even spread of time of flight (TOF) in the range of 3 - 5 lunar months. Breaking the TOF down further, the departure times are evenly spread through the month. However, arrival times are generally clustered around the  $\approx 120^\circ$  and  $\approx 300^\circ$  sun angles, as LETs necessitate the Sun tidal force to be exerted at a favorable orientation to raise the spacecraft's perigee to the Moon's semimajor axis, resulting in this temporal inflexibility.

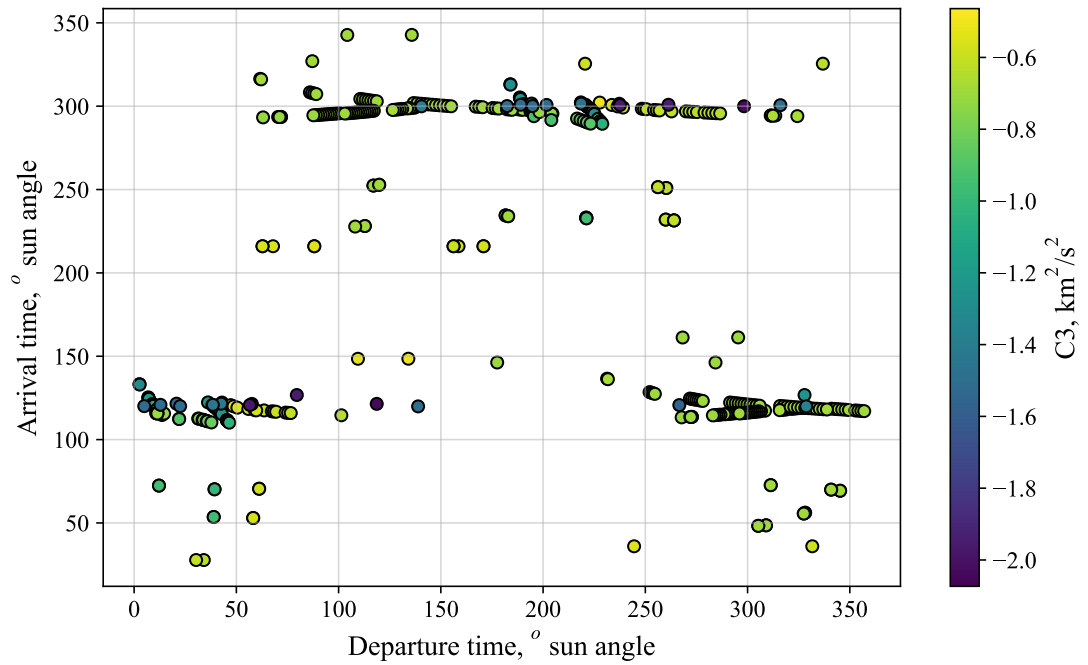
Using all of these trajectories in the logistics model would be impractical as it would create a huge commodity flow model. In addition, some trajectories are clearly better options than others: shorter TOF, low  $C_3$  options will always be better than longer TOF, high  $C_3$  options considering the small variations in LOI costs. So, these trajectories were down-selected, picking the most suitable trajectory for each vehicle for implementation in the logistics model.

The "most suitable" trajectory for a given vehicle was considered to be the one that results in its lowest launch mass, assuming a full-capacity payload. The launch mass was calculated for each vehicle by calculating its mass throughout a mission concept of operations (ConOps), in reverse chronological order from landing to launch, for each transfer:

- f*: Landing occurs at  $t = 4$  days into the lunar period (sun angle =  $48.8^\circ$ ). This is for simplified comparison with the direct lunar transfer, as the direct transfer (transfer time 3 days + 1 day loiter and landing) can then be assumed to launch at  $t = 0$  of the lunar period.
- 4: The spacecraft begins descent from LLO to the surface.  $\Delta V_{\text{desc}}$  is taken as 1.87 km/s in all cases.
- 3: The spacecraft loiters in LLO until it is time to begin the descent to the lunar surface. The loiter time  $T_{\text{loiter}}$  depends on the arrival time of the particular LET (see Figure 2b). For arrival times earlier than 3 days / sun angle  $36.6^\circ$ , descent begins during the same lunar



(a)  $C3$ , time of flight, and lunar orbit insertion cost for each of the generated low-energy transfers.



(b) Departure and arrival times of each of the generated low-energy transfers.

**Figure 2:** Key characteristics of the generated low-energy transfers.

period. Otherwise, the spacecraft loiters until the next period. For spacecraft with non-storable propellant types, boil-off during the loitering period is considered.

- 2: The spacecraft performs LOI after travelling the LET. LOI cost  $\Delta V_{LOI}$  is specific to the particular trajectory (see Figure 2a).
- 1: The spacecraft traverses the LET. Spacecraft with non-storable propellant types experience boil-off according to the TOF of the LET (see Figure 2a).
- 0: The spacecraft is injected into the LET by its launch vehicle. Here, the mass of the propellant expended by the launch vehicle is considered according to the launch vehicle's upper stages's  $I_{sp}$ . The  $\Delta V$  of the injection is calculated from the LET's C3, assuming that the maneuver starts in a 185 km low Earth orbit (LEO).

The propellant mass calculations associated with each stage of the ConOps, for each vehicle/LET combination, are as follows. The propellant used in the final descent is given in Equation (1).

$$m_{prop,4} = m_f \left( e^{\frac{\Delta V_{desc}}{I_{sp}g_0}} - 1 \right) \quad (1)$$

The propellant lost due to boil-off during LLO loitering is given by Equation (2), where  $\phi$  is propellant oxidizer mass ratio,  $\beta_{ox}$  is oxidizer fractional boil-off rate per day, and  $\beta_{fuel}$  is fuel fractional boil-off rate per day.

$$m_{prop,3} = m_{prop,4} \left( \phi (1 - \beta_{ox})^{-T_{loiter}} + (1 - \phi) (1 - \beta_{fuel})^{-T_{loiter}} \right) \quad (2)$$

Propellant used during LOI is given in Equation (3).

$$m_{prop,2} = (m_f + m_{prop,4} + m_{prop,3}) \left( e^{\frac{\Delta V_{LOI}}{I_{sp}g_0}} - 1 \right) \quad (3)$$

Propellant lost during the LET is given in Equation (4)

$$m_{prop,1} = (m_{prop,4} + m_{prop,3} + m_{prop,2}) \left( \phi (1 - \beta_{ox})^{-TOF} + (1 - \phi) (1 - \beta_{fuel})^{-TOF} \right) \quad (4)$$

Finally, the propellant expended by the launch vehicle during LTI is given by Equation (5), where  $I_{sp,LV}$  is the launch vehicle upper stage specific impulse.

$$m_{prop,0} = (m_f + m_{prop,4} + m_{prop,3} + m_{prop,2} + m_{prop,1}) \left( e^{\frac{\Delta V_{LTI}}{I_{sp,LV}g_0}} - 1 \right) \quad (5)$$

For comparison, propellant usage during direct transfers was calculated using the same process. The differences in propellant usage for some example vehicles between the direct transfer and each LET option are shown in Figure 3 (note that the change in propellant usage includes the savings in propellant expended by the LV upper stage and not the savings only to the lunar lander). Parameters associated with the vehicles will be detailed later in the case studies. The figure shows that two LET

options are useful: the minimum total  $\Delta V$  option is best for storable propellant vehicles, whilst a transfer with slight more  $\Delta V$  but significantly shorter total transfer time is best for cryogenic propellant options due to the impact of boil-off. These two trajectories are shown in Figure 4.

## Scheduling and Model Construction

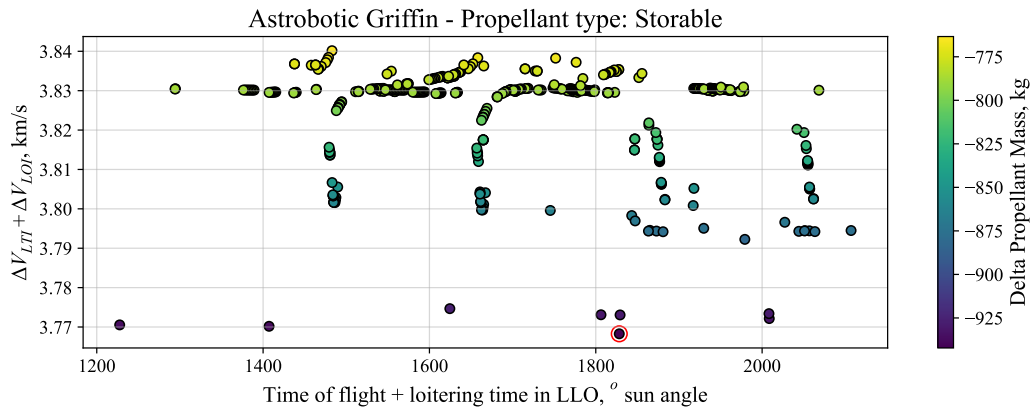
The model to be solved by the commodity flow MILP is constructed using inputs regarding the logistics network (including nodes, arcs, and costs), payload and their supplies/demands, and the available vehicles. The reader is referred to previous work for a complete description of the construction of the network with only direct transfers.<sup>18</sup>

*Inputs* The schedule optimizer requires, as input, certain information about the campaign payloads and vehicles. In addition to physical parameters such as masses, information about the schedule availability of the payloads and vehicles is of course required for the construction of scheduling constraints. For payloads, the parameters required are the mass, payload type, supply and demand nodes, the lower and upper bound of its allowed launch time, and any necessary precursor or co-payloads. For vehicles, the required physical parameters are dry mass, payload and propellant capacity, and specific impulse. The required scheduling parameters are the earliest date from which the vehicle is available and the frequency with which the vehicle can be used from then onwards. Each vehicle is assigned a “domain”  $\mathcal{D}$  - this is the set of arcs along which a vehicle is allowed to travel. Finally, sets of vehicle “stacks”  $\mathcal{S}$  are defined. These stack sets inform the algorithm of which vehicles can rendezvous and stack together.

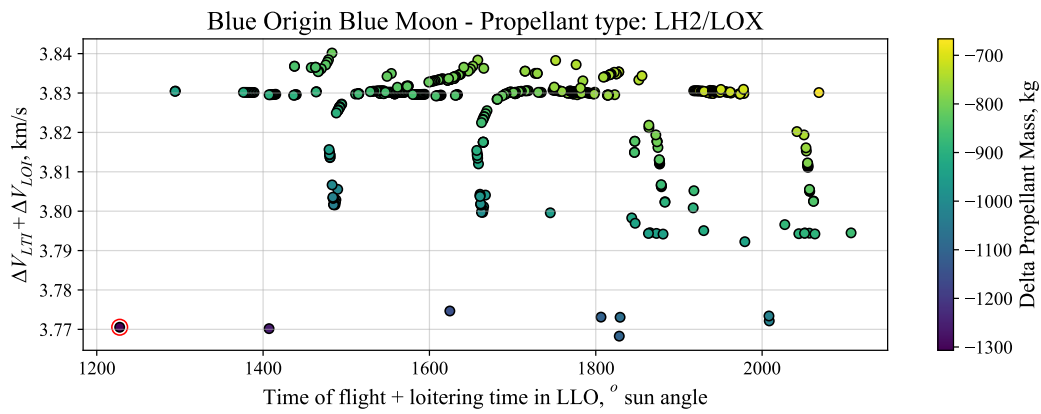
*Network Construction* The “baseline” network consists only of direct transfers. The costs considered in the network are the launch mass,  $\Delta V$ , discrete TOF, and real TOF. These values for the direct transfers and holdover arcs are listed in Table 1. Only launch mass features in the objective function - the other costs control the dynamics of the commodity flow. The discrete TOF is the number of lunar periods covered by the real TOF. Having established the process by which to find the LET that is most useful to each vehicle, those trajectories can now be added to the commodity flow network. The LET option offers a different route between two nodes in the network (from Earth to LLO) to the direct transfer, with different costs ( $\Delta V$  and TOF). One way of facilitating multiple routes between nodes is to include an additional “dummy” node, representing the alternative route. So, to include the LET options, an additional node was added to the network, which will be referred to as the “Weak Stability Boundary (WSB) node”. The WSB node has an arc *from* the Earth node, and an arc *to* the LLO node. The costs associated with each of these new nodes are shown in Table 2. The launch cost into the WSB node,  $Z_{LV,LET}$ , is the mass fraction of the LTI *relative* to launching into direct transfer from the same parking LEO, as per Equation (6). The time-expanded network including LETs is shown in Figure 5.

$$Z_{LV,LET} = \exp\left(\frac{\Delta V_{LET} - \Delta V_{direct}}{I_{sp,LV} g_0}\right) \quad (6)$$

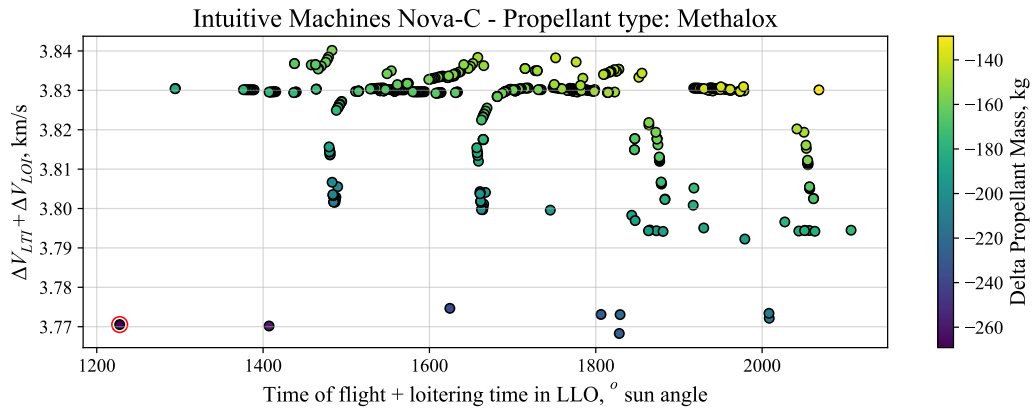
*Supply/Demand Matrix* The supply and demand requirements for each payload  $l$  of a campaign are determined by the decision vector  $\mathbf{x}(t_l)$  of a metaheuristic schedule optimizing algorithm. These decision vectors are chosen to solve the optimization problem outlined in Equation (7). The schedule optimization was performed using the pygmo<sup>24</sup> metaheuristic optimization python library.



(a) Storable propellant vehicle.



(b) Liquid hydrogen-oxygen propellant vehicle.



(c) Liquid methane-oxygen propellant vehicle.

**Figure 3:** Total time of flight (LET TOF + loitering time), total  $\Delta V$ , and propellant saving versus direct transfer, for three example vehicles with different propellant types. The LET with the greatest propellant saving for each type is circled in red.

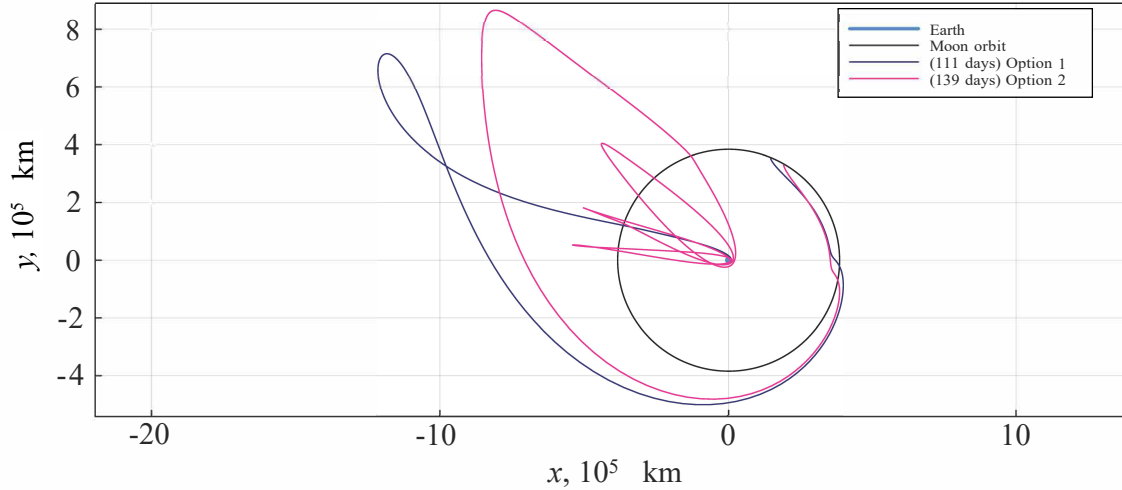


**Figure 4:** The two selected low-energy transfers plotted in the Sun-Earth rotating frame. “Option 1” is the shorter time-of-flight trajectory selected for vehicles with cryogenic propellant; “Option 2” is the cheaper but longer-TOF trajectory selected for vehicles with storable propellant.

**Table 1:** Costs associated with the direct transfers and holdover arcs.

Arc $[i, j]$	Launch cost $C$	$\Delta V$ (km/s)	Real TOF ( $^\circ$ sun angle)	Discrete TOF
Earth holdover [0, 0]	-	0	-	1
Earth - LLO [0,1]	1	0.89	36.57	0
LLO holdover [1,1]	-	0.15 per year (station-keeping) <sup>23</sup>	60.95 on even time step, 360 – 60.95 otherwise	1
LLO - Lunar surface [1,2]	-	1.87	12.19	0
Surface holdover [2,2]	-	0	36.57 on even time step, 360 – 36.57 otherwise	1
Surface - LLO [2,1]	-	1.87	12.19	0
LLO - Earth [1,0]	-	0.89	36.57	0

**Table 2:** Costs associated with the WSB arcs.

Arc $[i, j]$	Launch cost $C$	$\Delta V$	Real TOF	Discrete TOF
Earth - WSB [0,3]	$Z_{LV,LET}$	-	$TOF_{LET}$	$\lfloor TOF_{LET}/360 \rfloor$
WSB - LLO [3,1]	-	$\Delta V_{LTI}$	$T_{loiter}$	0 if $T_{loiter} \leq 36.6^\circ$ , 1 otherwise

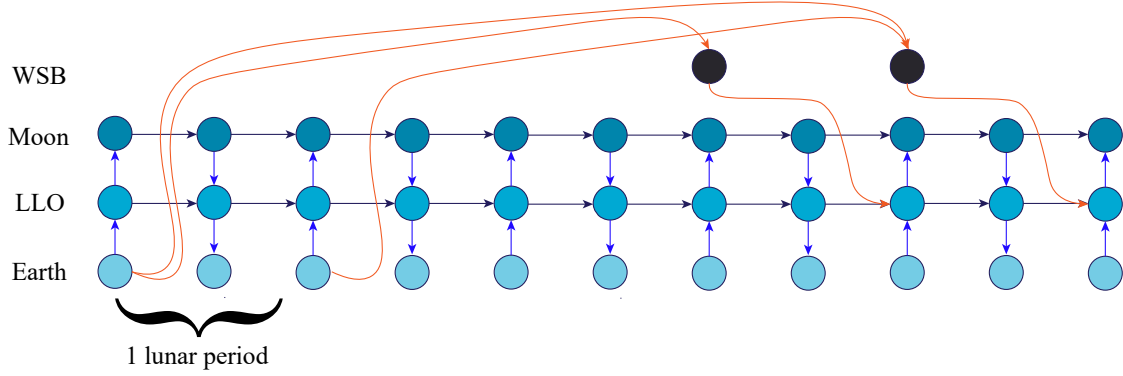


**Figure 5:** Time-expanded logistics network, showing direct transfer arcs (blue arrows), holdover arcs (black arrows) and LET arcs (orange arrows). Each lunar period is split into separate outbound and return arcs.

$$\begin{aligned}
 \min_{t_l} \quad & \mathcal{F}(\mathbf{x}(t_l), \mathcal{R}) \\
 \text{s.t.} \quad & t_q - t_l \leq 0 \quad \forall q \in \mathcal{P}_l \\
 & t_q - t_l < 0 \quad \forall q \in \mathcal{Q}_l \\
 & t_q - t_l = 0 \quad \forall q \in \mathcal{C}_l \\
 & t_{L,l} \leq t_l \leq t_{U,l}
 \end{aligned} \tag{7}$$

Where  $t_l$  is the arrival (demand) time of payload  $l$ ,  $\mathcal{R}$  is the set of programmatic requirements including payload and vehicle information, and  $\mathcal{P}_l$ ,  $\mathcal{Q}_l$ , and  $\mathcal{C}_l$  are the sets of soft pre-cursor (must arrive before or with), strict pre-cursor (must arrive before), and co- (must arrive with) payloads respectively.  $\mathcal{F}$  is the objective returned by the linear program.

When considering only direct transfers, the supply and demand times for a particular payload can occur within the same discrete time step, because a mission featuring direct transfers is less than one lunar period in length. When accounting for longer LETs though, this is no longer true - the times between supply (launch) and demand (landing) can be multiple lunar periods apart. Therefore, the matrix construction is changed so that the metaheuristic scheduler determines specifically the *demand* time for the campaign payloads. Then, the supply time is determined according to the follow rules:

- If the payload is crew, then the supply time is set to the same time step as the demand. This is to prevent crewed vehicles from using LETs - the long transfer times are not considered appropriate for crewed travel in these scenarios.
- If the payload follows a *return* flow direction (sourced at the Moon rather than Earth), then the supply time is set to the same time step as the demand. This is because no return low-energy trajectories have been considered.

**Table 3:** Definitions of the constants, indices, and variables used in the linear program.<sup>18</sup>

Constant	Description
$N$	Total number of vehicles designs
$I$	Total number of network nodes
$P_I$	Number of integer commodity types
$P_F$	Number of float commodity types
$P = P_I + P_F$	Total number of commodity types
$T_{LP}$	Total number of time steps in the linear program
Index	Description
$n \in [0, N)$	Vehicle
$i \in [0, I)$	Start node
$j \in [0, I)$	Final node
$p \in [0, P)$	Payload type
$io \in [0, 1]$	Into- or out-of-arc
$t \in [0, T_{LP})$	Time
Variables	Description
$x_{n,i,j,p,io,t}$	Quantity of commodity type $p$ , carried by vehicle $n$ , from node $i$ to node $j$ at time $t$ .
Terms	Description
$C_{n,i,p}$	Cost of launching commodity type $p$ , carried by vehicle $n$ , to node $i$ at time $t$ .
$d_{n,i,p,t}$	Demand matrix defining the supply (positive value) or demand (negative value) of commodity type $p$ , at node $i$ at time $t$ .
$Z_{n,i,j,t}$	Propellant mass fraction associated with vehicle $n$ travelling from node $i$ to node $j$ at time $t$ .
$c$	Crew consumables consumption rate
$\rho$	ISRU propellant production rate
$\tau_{n,i,j,t}$	Real time of flight between node $i$ and node $j$ at discrete time index $t$ when using vehicle $n$
$T_{n,i,j,t}$	Discrete time of flight between node $i$ and node $j$ at discrete time index $t$ when using vehicle $n$
$\mathcal{E}_{i,j,t}$	Boolean variable defining whether the arc from node $i$ to node $j$ exists. at time $t$ . Outbound arcs exist only on even time steps and return arcs exist only on odd time steps.

- Otherwise, the supply time is set to the time step equal to the demand time minus the longest LET discrete TOF, as long as this does not violate programmatic constraints (for example, if this would supply the payload earlier than the programmatic requirements state as it's earliest allowed supply date).
- Vehicles are supplied one-at-a-time, starting with their earliest-available time, and subsequently according to their minimum launch frequency.

### Logistics Linear Program

The mixed-integer linear program finds the minimum launch mass commodity flow that satisfies the model constructed as described above. The various constants, indices, and variables used to construct and solve the linear program are summarized in Table 3.

Shown in Equation (8), the objective function of the MILP is to minimize the cost of launching

all of the campaign material into lunar transfer.

$$\min_x f(x) = \sum_t \sum_n \sum_p \sum_j C_{p,n,j} x_{n,0,1,p,0,t} \quad (8)$$

The commodity flow is subject to a number of constraints. First, Equations (9) and (10), impose the supply or demand at each node. The difference between the total amount of commodity flowing *into* a node from all others and the amount of the same commodity *leaving* the node to all others, is limited by the supply or demand. Note that vehicles must satisfy the demand/supply of their type or within their allowed stacks, whilst for all other payloads, only the sum of the payload delivered by all logistics vehicles is considered. A vehicle stack is a collection of individual vehicles transported together, e.g., a lander carrying an ascent vehicle. The functionality and implementation of vehicle stacking is described in the previous work, and is based on the ontologies developed by Trent,<sup>25</sup> Edwards *et al*,<sup>26</sup> and Downs.<sup>27</sup> The second constraint enforces vehicle payload capacities. Note that the mass of the *in-situ* resource utilization (ISRU) plants (index  $p = 2$ ) is excluded from the capacity for holdover arcs and the lunar surface as they are intended to remain in place on the lunar surface independent of the movement of logistics vehicles. The third constraint imposes the propellant capacity constraints.

The fourth constraint enforces the dynamics surrounding the various commodities. Firstly, Equation (14) governs the maintenance supplies (index  $p = 3$ ) associated with ISRU infrastructure. Maintenance supplies equal to 10% of the mass of ISRU infrastructure on the lunar surface per year was required. Equation (15) shows how crew consumables (index  $p = 4$ ) are consumed at a constant rate. 8.655 kg of consumables per crew member per day was required.<sup>13</sup> Equations (16) and (17) describe oxidizer (index  $p = 6$ ) and fuel (index  $p = 7$ ) consumption when traveling over arcs. All arcs suffer from boil-off, which is modeled as a fractional loss rate  $\beta^\tau$ . Loss rates of 0.025 % per day for liquid oxygen,<sup>28</sup> 0.1 % per day for liquid hydrogen,<sup>28</sup> and 0.08% per day for liquid methane,<sup>29</sup> were used throughout the case studies. Holdover arcs on the lunar surface ( $i = 2$ ) allow for refilling oxidizer from ISRU-produced propellant, produced at a constant rate  $\rho$ . A production rate 0.00153 kg of oxygen per day per kg of ISRU infrastructure present on the surface was used.<sup>18</sup> Equation (18) states that other commodities are simply conserved across arcs.

The final constraint ensures that commodities only flow along arcs that exist at the current time step, and that vehicles remain within their domains. The MILP commodity flow model was constructed using the Pyomo python library<sup>30,31</sup> and optimization was carried out using the Gurobi optimization software.<sup>32</sup>

$$c_{1a}(x) : \sum_{n \in \mathcal{S}_n} \sum_j (x_{n,i,j,p,0,t} - x_{n,j,i,p,1,t-T_{n,j,i,t}}) \leq d_{n,i,p,t} \quad \forall \mathcal{S}, t \quad \text{if } p = 0 \quad (9)$$

$$c_{1b}(x) : \sum_n \sum_j (x_{n,i,j,p,0,t} - x_{n,j,i,p,1,t-T_{n,j,i,t}}) \sum_n \leq d_{n,i,p,t} \quad \forall t \quad \text{if } p > 0 \quad (10)$$

$$c_2(x) : \begin{cases} 100x_{n,i,j,1,0,t} + \sum_{p=2}^5 x_{n,i,j,p,0,t} \leq x_{n,i,j,0,0,t} m_{\text{pay},n}, & \forall n, t \quad \text{if } i \neq j \text{ or } i \neq 2 \\ 100x_{n,i,j,1,0,t} + \sum_{p=3}^5 x_{n,i,j,0,0,t} \leq x_{n,i,j,0,0,t} m_{\text{pay},n}, & \forall n, t \quad \text{otherwise} \end{cases} \quad (11)$$

$$c_{3a}(x) : \quad x_{n,i,j,6,0,t} \leq x_{n,i,j,0,0,t} \phi_n m_{\text{prop},n} \quad \forall n, t, i, j \quad (12)$$

$$c_{3b}(x) : \quad x_{n,i,j,7,0,t} \leq x_{n,i,j,0,0,t} (1 - \phi_n) m_{\text{prop},n} \quad \forall n, t, i, j \quad (13)$$

$$c_{4a}(x) : \quad \sum_n x_{n,3,3,3,1,t} - \sum_n x_{n,3,3,3,0,t} + \mu \tau_{3,3,t} x_{n,3,3,2,1,t} = 0 \quad \forall t \quad (14)$$

$$c_{4b}(x) : \quad x_{n,i,j,4,1,t} - x_{n,i,j,4,0,t} + c \tau_{i,j,t} x_{n,i,j,0,1,t} = 0 \quad \forall n, t, i, j \quad (15)$$

$$c_{4c}(x) : \quad \begin{cases} (1 - \beta_{\text{ox},n})^{\tau_{i,j,t}} x_{n,i,j,6,1,t} - x_{n,i,j,6,0,t} + & \forall n, t, i, j \quad \text{if } i \neq 2 \\ \phi_n Z_{n,i,j} \left( x_{n,i,j,0,0,t} m_{\text{dry},n} + 100 x_{n,i,j,1,0,t} + \sum_{p=2}^7 \right) = 0 & \\ (1 - \beta_{\text{ox},n})^{\tau_{i,j,t}} x_{n,i,j,6,1,t} - x_{n,i,j,6,0,t} + \rho \tau_{i,j,t} = 0 & \forall n, t, i, j \quad \text{if } i = j = 2 \end{cases} \quad (16)$$

$$c_{4d}(x) : \quad (1 - \beta_{\text{f},n})^{\tau_{i,j,t}} x_{n,i,j,7,1,t} - x_{n,i,j,7,0,t} + \\ (1 - \phi_n) Z_{n,i,j} \left( x_{n,i,j,0,0,t} m_{\text{dry},n} + 100 x_{n,i,j,1,0,t} + \sum_{p=2}^7 \right) = 0 \quad \forall n, t, i, j \quad (17)$$

$$c_{4e}(x) : \quad x_{n,i,j,p,1,t} - x_{n,i,j,p,0,t} = 0 \quad \forall n, t, i, j \quad \forall p \in \{0, 1, 3, 4, 5\} \quad (18)$$

$$c_5(x) : \quad x_{n,i,j,p,io,t} = \begin{cases} 0 \quad \forall i, j, p, io \quad \text{if } [i, j] \notin \mathcal{D}_n \\ 0 \quad \forall n, p, io, t \quad \text{if } \mathcal{E}_{i,j,t} = 0 \\ \text{unconstrained otherwise} \end{cases} \quad (19)$$

## CASE STUDIES

Next, the LET logistics network is applied to some previously analyzed<sup>18</sup> lunar exploration campaigns to find if expanding the choice of trajectories with the inclusion of LETs can reduce the overall launch mass, beyond the optimization of schedule and commodity flow assuming only direct transfers. First, the Commercial Lunar Payload Services (CLPS) campaign, consisting of payload deliveries to the lunar surface via commercial landers, is analyzed. Then, the more complex Artemis crewed lunar surface exploration campaign is studied.

**Table 4:** Payload data used in the CLPS analysis. Data quoted from sources where possible, and best approximations are made otherwise. First lunar period  $t = 0$  is taken as December 2022. Adapted from Gollins *et al.*<sup>17</sup>

#	Name	Quantity	$i$	$j$	$t_L$	$t_U$	$\mathcal{C}$
0	First shared payloads <sup>33</sup>	14	0	2	0	12	
1	First shared payloads	14	0	2	0	12	
2	CLPS-1 <sup>33,34</sup>	50	0	2	0	12	0
3	Lunar Flashlight	12	0	2	0	12	
4	CLPS-2 <sup>33,34</sup>	50	0	2	0	12	1
5	CLPS-3 / PRIME-1 <sup>34,35</sup>	36	0	2	7	12	
6	CLPS-4 <sup>34</sup>	300	0	2	13	13	
7	CLPS-5 <sup>34</sup>	50	0	2	13	24	
8	VIPER <sup>34,36</sup>	430	0	2	12	25	
9	Mare Crisium mission <sup>34,37</sup>	94	0	2	13	25	
10	Schrödinger mission <sup>34,38</sup>	95	0	2	25	36	

### CLPS Campaign

The CLPS campaign is a series of science payloads contracted out by NASA to be delivered to the lunar surface over the coming years, preceding the Artemis 3 crewed surface mission. The payloads and vehicles considered by this analysis are summarized in Tables 4 and 5 respectively. A subset of these vehicles are those used demonstratively in Figure 3. The vehicles with  $I_{sp} < 370$  are considered to use storable propellant, those with  $I_{sp}$  in the range 370 - 420 are considered to use cryogenic liquid methane/oxygen propellant, and those with  $I_{sp} \geq 370$  are considered to use cryogenic liquid hydrogen/oxygen propellant.

Previous analysis<sup>18</sup> found that the total launch mass of the assumed baseline schedule, with only direct transfers, was 19061 kg, and that the total launch mass with optimized schedule was 14207 kg. In the direct-transfer-only model, supply and demand times were set to be within the same discrete time step. In the LET logistics model, this is not always the case, due to the long time of flight of LETs. Therefore, for a proper comparison, the baseline schedule was first re-analyzed *without* the LET option, but with the supply times set to earlier time steps as required *with* the LET option, where possible. This gives an isolated understanding of the impact that the required relaxation of the schedule associated with implementing long-TOF trajectories has on the commodity flow solution. In this relaxed-schedule case, the total launch mass was found to be 18366 kg.

Next, the baseline CLPS schedule was evaluated again, this time with the choice of LETs enabled. The total launch mass reduced to 18193 kg. The resulting commodity flow is shown in Figure 6. The vehicles and payloads using the LETs are highlighted in red - two payloads were assigned to these trajectories, resulting in the 200kg mass saving across the campaign. One of the choices for LET usage was relatively obvious: a payload that stood alone in the overall schedule, and had loose scheduling requirements allowing for the long time of flight. The other, though, was not a clear choice, as that particular payload fell, in terms of schedule, closer other payloads for which the optimizer opted to reduce mass by ride-sharing.

Having established an updated baseline scenario to draw comparison to, the metaheuristic sched-



**Table 5:** Vehicle data used in the CLPS analysis. Data quoted from sources where possible, and best approximations made otherwise. First lunar period  $t = 0$  is taken as December 2022. Adapted from Gollins *et al.*<sup>17</sup>

#	Name	$m_{pay}$ , kg	$m_{prop}$ , kg	$m_{dry}$ , kg	$I_{sp}$ , s	LV $I_{sp}$ , s	$t_F$	$t_L$	$\mathcal{D}$
0	Astrobotic <sup>39</sup> "Peregrine"	90	720	470	340	453.8 <sup>40</sup>	12	1	[0,0], [0,1], [1,2], [1,1], [2,2], [0,3], [3,1]
1	Astrobotic <sup>41,42</sup> "Griffin"	630	3320	1950	340	453.8 <sup>40</sup>	12	24	[0,0], [0,1], [1,2], [1,1], [2,2], [0,3], [3,1]
2	B.O. <sup>43,44</sup> "Blue Moon"	4500	6350	2150	420	450	12	24	[0,0], [0,1], [1,2], [1,1], [2,2], [0,3], [3,1]
3	ispace S1 <sup>45</sup>	30	700	300	340	348	12	0	[0,0], [0,1], [1,2], [1,1], [2,2], [0,3], [3,1]
4	Draper <sup>46</sup> /ispace S2	500	3380	2120	340	348	12	13	[0,0], [0,1], [1,2], [1,1], [2,2], [0,3], [3,1]
5	Firefly <sup>47</sup> "Blue Ghost"	155	3380	2470	340	348	12	13	[0,0], [0,1], [1,2], [1,1], [2,2], [0,3], [3,1]
6	I.M. <sup>48</sup> "Nova-C"	100	1010	790	370	348	6	0	[0,0], [0,1], [1,2], [1,1], [2,2], [0,3], [3,1]
7	L.M. <sup>49</sup> "McCandless"	350	3380	2270	340	348	12	48	[0,0], [0,1], [1,2], [1,1], [2,2], [0,3], [3,1]
8	M.E. MX-1 <sup>50</sup> "Scout"	30	150	70	320	348	12	48	[0,0], [0,1], [1,2], [1,1], [2,2], [0,3], [3,1]

ule optimizer was used to find the optimal schedule with LETs enabled. Using a population size of 20 and a mutation propability of 0.05, the best found solution after 50 generations was 14210 kg. This is approximately equal to the previously best found solution with only direct transfers, with the minor deviation attributed to model updates. Indeed, shown in Figure 7, the commodity flow produced by this optimal schedule does not include any LET choices. This demonstrates that, when the schedule allows, maximizing ride-sharing provides a larger benefit in mass savings than staggering launches in order to use long-TOF LETs. This is possible in this CLPS campaign analysis because the scheduling requirements are not overly constraining.

## Artemis Program

Finally, the effect that the introduction of LETs to the logistics of a campaign with more scheduling complexity was studied. As an example, an extended Artemis lunar surface exploration campaign based on the Global Exploration Roadmap plans<sup>51,52</sup> was analyzed. The sets of payloads and vehicles implemented in this campaign are listed in Tables 6 and 7 respectively. As well as the vehicle listed here, the ISECG vehicles and Mk 2 vehicles are allowed to form stacks amongst themselves. The start of the campaign  $t = 0$  is not strictly defined, but is assumed to be in the early 2030's. It should also be noted that ISRU infrastructure is enabled in this analysis.

The combination of long campaign length with the addition of long-TOF trajectories results in a commodity flow model with many discrete time steps. This results in rapidly increasing solve times for the MILP optimizer (in fact, this is one of the reasons for using a metaheuristic schedule optimizer instead of passing the full schedule solution space to the MILP<sup>18</sup>). To avoid this issue, some measures were taken to reduce the scale of the model. First, the list of vehicles in Table 7 has been trimmed of the smaller CLPS vehicles that would be less useful in the Artemis program,

**Table 6:** Payload data used in the Artemis surface exploration program analysis. Adapted from Gollins *et al.*<sup>17,18</sup>

#	Name	Type Index	Quantity	$i$	$j$	$t_L$	$t_U$	$\mathcal{P}$	$\mathcal{Q}$	$\mathcal{C}$
0	Power Plant element	5	1500	0	2	0	48			
1	Artemis 7 Crew	1	4	0	1	0	48	0		
2	Artemis 7 Crew Landing	1	4	1	2	0	48			1
3	Artemis 7 Crew Ascent	1	4	2	1	0	48		2	
4	Artemis 7 Crew Return	1	4	1	0	0	48			3
5	Sample return	5	200	2	0	0	48			
6	Habitat	5	4500	0	2	0	54			
7	Artemis 8 Crew	1	4	0	1	0	54	6	4	
8	Artemis 8 Crew Landing	1	4	1	2	0	54			7
9	Artemis 8 Crew Ascent	1	4	2	1	0	54		8	
10	Artemis 8 Crew Return	1	4	1	0	0	54			9
11	Sample return	5	200	2	0	0	54			
12	Artemis 9 Crew	1	4	0	1	12	60		10	
13	Artemis 9 Crew Landing	1	4	1	2	12	60			12
14	Artemis 9 Crew Ascent	1	4	2	1	12	60		13	
15	Artemis 9 Crew Return	1	4	1	0	12	60			14
16	Sample return	5	200	2	0	12	60			
17	Pressurised Rover	5	4500	0	2	0	66			
18	Pressurised Rover	5	4500	0	2	0	66			
19	Artemis 10 Crew	1	4	0	1	24	66	17, 18	15	
20	Artemis 10 Crew Landing	1	4	1	2	24	66			19
21	Artemis 10 Crew Ascent	1	4	2	1	24	66		20	
22	Artemis 10 Crew Return	1	4	1	0	24	66			21
23	Sample return	5	200	2	0	24	66			
24	Artemis 11 Crew	1	4	0	1	36	72		22	
25	Artemis 11 Crew Landing	1	4	1	2	36	72			24
26	Artemis 11 Crew Ascent	1	4	2	1	36	72		25	
27	Artemis 11 Crew Return	1	4	1	0	36	72			26
28	Sample return	5	200	2	0	36	72			
29	Artemis 12 Crew	1	4	0	1	48	84		27	
30	Artemis 12 Crew Landing	1	4	1	2	48	84			29
31	Artemis 12 Crew Ascent	1	4	2	1	48	84		30	
32	Artemis 12 Crew Return	1	4	1	0	48	84			31
33	Sample return	5	200	2	0	48	84			
34	Fission Power Plant	5	4500	0	2	48	84			
35	Habitat	5	4500	0	2	48	84			
36	Artemis 13 Crew	1	4	0	1	60	96	34, 35	32	
37	Artemis 13 Crew Landing	1	4	1	2	60	96			36
38	Artemis 13 Crew Ascent	1	4	2	1	60	96		37	
39	Artemis 13 Crew Return	1	4	1	0	60	96			38
40	Sample return	5	200	2	0	60	96			
41	Artemis 14 Crew	1	4	0	1	72	96		39	
42	Artemis 14 Crew Landing	1	4	1	2	72	96			41
43	Artemis 14 Crew Ascent	1	4	2	1	72	96		42	
43	Artemis 14 Crew Return	1	4	1	0	72	96			43
44	Sample return	5	200	2	0	72	96			

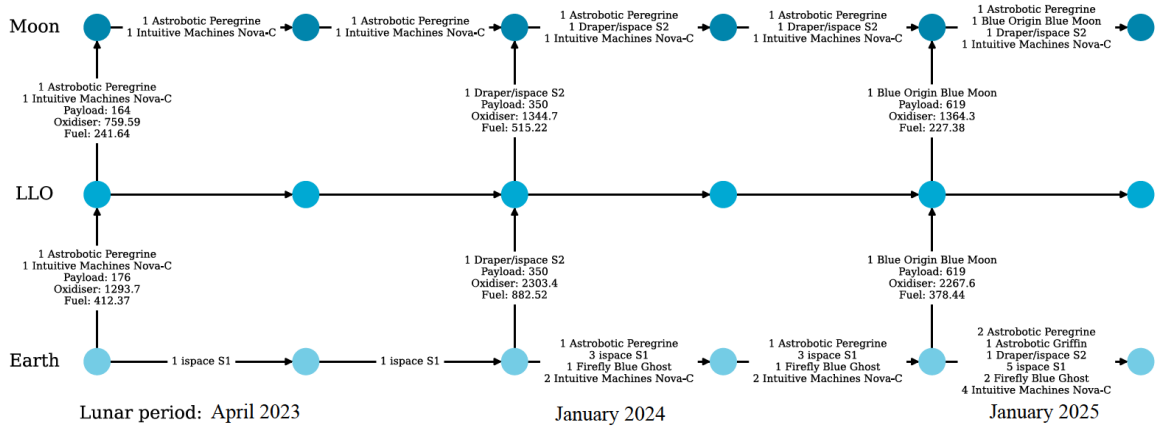


**Figure 7:** Commodity flow for the CLPS campaign with optimized schedule. Lunar periods are indicated by the approximate corresponding calendar month.

**Table 7:** Vehicle data used in the Artemis surface exploration program analysis. ISECG vehicles based on Guidi *et al.*,<sup>53</sup> MK2 versions based on Landgraf.<sup>52</sup> Adapted from Gollins *et al.*<sup>17,18</sup>

#	Name	$m_{pay}$ , kg	$m_{prop}$ , kg	$m_{dry}$ , kg	$I_{sp}$ , s	LV $I_{sp}$ , s	$t_F$	$t_L$	$\mathcal{D}$
0	Astrobotic <sup>41,42</sup> "Griffin"	630	3320	1950	340	453.8 <sup>40</sup>	12	0	[0,0], [0,1], [1,2], [1,1], [2,2], [0,3], [3,1]
1	B.O. <sup>43,44</sup> "Blue Moon"	4500	6350	2150	420	450	6	0	[0,0], [0,1], [1,2], [1,1], [2,2], [0,3], [3,1]
2	Draper <sup>46</sup> /inspace S2	500	3380	2120	340	348	12	0	[0,0], [0,1], [1,2], [1,1], [2,2], [0,3], [3,1]
3	I.M. <sup>48</sup> "Nova-C"	100	1010	790	370	348	6	0	[0,0], [0,1], [1,2], [1,1], [2,2], [0,3], [3,1]
4	ESA EL3 <sup>54</sup>	1800	5580	2520	340	457 <sup>55</sup>	36	0	[0,0], [0,1], [1,2], [1,1], [2,2], [0,3], [3,1]
5	ISECG lander <sup>53</sup>	9000	23660	9340	340	460.1 <sup>40</sup>	12	0	[0,0], [0,1], [1,2], [1,1], [2,2], [0,3], [3,1]
6	ISECG ascender	500	10000	1000	340	460.1 <sup>40</sup>	12	0	[0,0], [2,2], [2,1]
7	Orion	11800	22000	16520	316	460.1 <sup>40</sup>	1	0	[0,0], [0,1], [1,1], [1,0]
8	MK2 ISECG lander	11390	23660	9340	370	460.1 <sup>40</sup>	12	0	[0,0], [0,1], [1,2], [1,1], [2,2], [0,3], [3,1]
9	MK2 ISECG ascender	500	10000	1000	370	460.1 <sup>40</sup>	12	0	[0,0], [2,2], [2,1]

which largely consists of more massive payloads. Second, the metaheuristic schedule optimization was performed with LETs disabled, so that there is only a maximum of one discrete time index per payload, rather than the maximum of five time-steps required to represent an LET. Then, with improved schedules for the direct-transfer-only ConOps identified, that solution is then re-evaluated with the LET network enabled. This search method for optimality works with the assumptions that the direct-transfer-only solution space is a subset of the LET-enabled solution space; that the objective of the LET-enabled problem is better than, or at least equal to, the objective of the direct-only problem; and that the transformation from the direct-only space to LET-enabled space maintains the shape of the objective function. That is to say that, any optima maintain the same positions in the solution spaces of the two problems. The first of these two statements are clearly true - enabling additional trajectory options cannot make a solution worse, as the MILP solver can simply choose not to use those additional options if they are sub-optimal. The latter statement is difficult to prove, but the assumption is considered acceptable in this study as it is anyway difficult to claim global optimality of a discrete categorical optimization problem using metaheuristics with finite computing time, and therefore this method only searches for *improved* solutions compared to initial guesses, and not necessarily the strict global optimum.

The schedule optimization was performed using 2 parallel populations of 20 individuals each evolved through 120 generations with a mutation chance of 0.01. The best found direct-transfer-only solution had a total launch mass of 604220 kg. Re-evaluating this same solution with LETs enabled, the objective improved to 589890 kg. The commodity flow is complex and therefore not included here as a figure, but it produced 6 distinct missions that utilized LETs. One of each of those were in support of Artemis missions 8, 9, 10, 11, 13, and 14. Neither Artemis 7 or 12 relied on any LETs.

Prior to the Artemis 8 landing, the crew habitat is launched, along with 240 kg of crew consumables and 550 kg of maintenance supplies, on an ISECG descent/ascent vehicle stack. When this vehicle arrives in lunar orbit, the Artemis 8 crew is launched on an Orion spacecraft, accompanied by an upgraded Mk2 stack, and the two sets of vehicles land together. The Artemis 9 mission is supported by an ISECG stack launched into an LET, carrying 100 kg of crew supplies. Again, this supporting mission meets the crew in lunar orbit, but this time supplies carried along the LET are transferred to the Orion capsule that awaits the crew's return in lunar orbit, for use on the return leg of the journey. Artemis 10, like 8, has a large supporting payload: two 4500 kg pressurized rovers. These are transporting via LET aboard a Mk2 lander/ascent stack, along with 270 kg of maintenance and 170 kg of crew supplies. Artemis 11 has two supporting missions associated with it. 550 kg of maintenance and 350 kg of crew supplies are launched on a Mk2 stack along the shorter TOF LET, and meet with the crew in lunar orbit. At the same time, a Mk1 stack is launched along the longer TOF LET. The crewed mission here is two months long, so the Mk1 stack is able to land and assist with the crew's return. Before Artemis 13, 8000 kg of the 9000 kg of pressurized rovers\* are launched aboard a Mk1 ISECG vehicle stack, travelling via the longer-TOF LET. One month later, the remaining 1000 kg of payload, plus 300 kg of maintenance supplies and 170 kg crew consumables are launched aboard a Mk2 vehicle stack. Due to the different TOFs, these vehicles meet in lunar orbit. There, they also meet the Artemis 13 crew, and both sets of vehicles land together. Finally, Artemis 14 is supported by a Mk2 vehicle stack that travels to lunar orbit via LET, carrying

---

\*Note that payloads are considered to be continuous values in the MILP - there is no problem in dividing them in this manner. Presumably, this commodity flow would work by dismantling one of the rovers and re-assembling it on the lunar surface.

170 kg of crew supplies with it.

In summary, for this particular Artemis phase 2B ConOps, LETs have proven useful for two purposes. Firstly, it is cheaper to transport the various supporting payloads along LETs. Secondly, regardless of the necessity for supporting payloads, it is sometimes beneficial for the lander and ascent vehicle stacks to launch before the crew, travel along the LET and rendezvous with the crew in lunar orbit. In fact, this makes a lot of sense for future Artemis plans involving in-orbit assembly, as the un-crewed elements would always launch before the crew themselves, irrespective of the path that they take.

## CONCLUSION

This paper has discussed the potential advantages of considering alternatives to direct transfers in translunar logistics. In particular, weak stability boundary (low-energy) transfers have been implemented into existing logistics optimization methods and demonstrated with real-world-based case studies. It has been found that LETs can be effective methods of reducing the overall launch mass of a lunar exploration campaign, if the schedule allows for the longer time-of-flights.

However, in situations where multiple small payloads are scheduled to be delivered to their destination within overlapping, but not identical, time windows, ride-sharing along direct transfers is a more effective solution to reducing mass whilst meeting scheduling constraints compared to separate launches into weak stability boundary trajectories. LETs are the most effective option either for stand-alone payloads that are not constrained by time-of-flight, or for large payloads that require a dedicated vehicle.

## REFERENCES

- [1] G. R. Woodcock, "Logistics support of lunar bases," *Acta Astronautica*, Vol. 17, Jul 1988, p. 717–738, 10.1016/0094-5765(88)90186-5.
- [2] G. Fasano, "Mixed integer linear approach for the space station on-orbit resources re-supply," *AIRO 96 Annual Conference Proceedings*, Perugia, Italy, Sep 1996.
- [3] G. Fasano and R. Provera, "A traffic model for the space station on-orbit re-supply problem," *The International Society of Logistics Engineering (SOLE), Logistics National Conference Proceedings*, Turin, Italy, Oct 1997.
- [4] E. Gralla, S. Shull, and O. de Weck, "A Modeling Framework for Interplanetary Supply Chains," *Space 2006*, San Jose, California, American Institute of Aeronautics and Astronautics, Sep 2006, 10.2514/6.2006-7229.
- [5] C. Taylor, D. Klabjan, D. Simchi-levi, M. Song, and O. De Weck, "Modeling Interplanetary Logistics: A Mathematical Model for Mission Planning," *AIAA Journal*, Jun 2006, 10.2514/6.2006-5735.
- [6] P. Grogan, H. Yue, and O. De Weck, "Space Logistics Modeling and Simulation Analysis using SpaceNet: Four Application Cases," *AIAA SPACE 2011 Conference & Exposition*, Long Beach, California, American Institute of Aeronautics and Astronautics, Sep 2011, 10.2514/6.2011-7346.
- [7] K. Ho, O. de Weck, J. Hoffman, and R. Shishko, "Dynamic modeling and optimization for space logistics using time-expanded networks," *Acta Astronautica*, Vol. 105, Oct 2014, 10.1016/j.actaastro.2014.10.026.
- [8] T. Ishimatsu, O. L. de Weck, J. A. Hoffman, Y. Ohkami, and R. Shishko, "Generalized Multicommodity Network Flow Model for the Earth–Moon–Mars Logistics System," *Journal of Spacecraft and Rockets*, Vol. 53, Jan 2016, p. 25–38, 10.2514/1.A33235.
- [9] G. Blosssey, "A Stochastic Modeling Approach for Interplanetary Supply Chain Planning," *Space: Science & Technology*, Vol. 3, Jan 2023, p. 0014, 10.34133/space.0014.
- [10] T. Sarton du Jonchay, H. Chen, M. Isaji, Y. Shimane, and K. Ho, "On-Orbit Servicing Optimization Framework with High- and Low-Thrust Propulsion Tradeoff," *Journal of Spacecraft and Rockets*, Vol. 59, Jan 2022, p. 33–48, 10.2514/1.A35094.
- [11] Y. Shimane, N. Gollins, and K. Ho, "Orbital Facility Location Problem for Satellite Constellation Servicing Depots," 2023. arXiv:2302.12191.

- [12] J. A. Tepper, Y. Fassi, T. Sarton du Jonchay, K. Ho, and Y. Shimane, "Optimization and Modeling of Active Debris Removal using a Time-Expanded Network," *ASCEND 2022*, Las Vegas, Nevada, American Institute of Aeronautics and Astronautics, Oct 2022, 10.2514/6.2022-4245.
- [13] H. Chen and K. Ho, "Integrated Space Logistics Mission Planning and Spacecraft Design with Mixed-Integer Nonlinear Programming," *Journal of Spacecraft and Rockets*, Vol. 55, Mar 2018, p. 365–381, 10.2514/1.A33905.
- [14] H. Chen, T. Sarton du Jonchay, L. Hou, and K. Ho, "Multifidelity Space Mission Planning and Infrastructure Design Framework for Space Resource Logistics," *Journal of Spacecraft and Rockets*, Vol. 58, Mar 2021, p. 538–551, 10.2514/1.A34666.
- [15] M. Isaji, Y. Takubo, and K. Ho, "Multidisciplinary Design Optimization Approach to Integrated Space Mission Planning and Spacecraft Design," *Journal of Spacecraft and Rockets*, Vol. 59, Nov 2021, p. 1660–1670, 10.2514/1.A35284.
- [16] Y. Takubo, H. Chen, and K. Ho, "Hierarchical Reinforcement Learning Framework for Stochastic Spaceflight Campaign Design," *Journal of Spacecraft and Rockets*, Vol. 59, Mar 2022, p. 421–433, 10.2514/1.A35122.
- [17] N. J. Gollins, M. Isaji, Y. Shimane, and K. Ho, "A Heuristic Method for Determining Payload-to-Vehicle Assignment & Launch Order for Multi-Vehicle Exploration Campaigns," *AIAA SCITECH 2023 Forum*, National Harbor, Maryland, American Institute of Aeronautics and Astronautics, Jan 2023, 10.2514/6.2023-1965.
- [18] N. Gollins and K. Ho, "Hierarchical Space Exploration Campaign Schedule Optimization With Ambiguous Programmatic Requirements," 2023. arXiv:2308.00632.
- [19] B. B. Jagannatha, J.-B. H. Bouvier, and K. Ho, "Preliminary Design of Low-Energy, Low-Thrust Transfers to Halo Orbits Using Feedback Control," *Journal of Guidance, Control, and Dynamics*, Vol. 42, Feb 2019, p. 260–271, 10.2514/1.G003759.
- [20] B. B. Jagannatha and K. Ho, "Event-Driven Network Model for Space Mission Optimization with High-Thrust and Low-Thrust Spacecraft," *Journal of Spacecraft and Rockets*, Vol. 57, May 2020, p. 446–463, 10.2514/1.A34628.
- [21] W. S. Koon, M. W. Lo, J. E. Marsden, and S. D. Ross, "Low Energy Transfer to the Moon," *Celestial Mechanics and Dynamical Astronomy*, Vol. 81, Sep 2001, p. 63–73, 10.1007/978-94-017-1327-6.8.
- [22] Y. Shimane, "Periapsis Targeting with Weak Stability Boundary Transfers for Orbiting Around Planetary Moons," *AAS/AIAA Space Flight Mechanics Meeting*, 2021, pp. 1–12.
- [23] M. Beckman and R. Lamb, *Stationkeeping for the Lunar Reconnaissance Orbiter (LRO)*. NASA, 2007.
- [24] F. Biscani and D. Izzo, "A parallel global multiobjective framework for optimization: pagmo," *Journal of Open Source Software*, Vol. 5, No. 53, 2020, p. 2338, 10.21105/joss.02338.
- [25] D. Trent, *Integrated Architecture Analysis and Technology Evaluation for Systems of Systems Modeled at the Subsystem Level*. PhD thesis, Georgia Institute of Technology, Atlanta, GA, Nov 2017.
- [26] S. J. Edwards, D. Trent, M. J. Diaz, and D. N. Mavris, "A Model-Based Framework for Synthesis of Space Transportation Architectures," *2018 AIAA SPACE and Astronautics Forum and Exposition*, Orlando, FL, American Institute of Aeronautics and Astronautics, Sep 2018, 10.2514/6.2018-5133.
- [27] C. Downs, A. Prasad, B. E. Robertson, and D. N. Mavris, "A Spaceflight Logistics Approach to Modeling Novel Vehicle Concepts," *AIAA SCITECH 2023 Forum*, National Harbor, MD & Online, American Institute of Aeronautics and Astronautics, Jan 2023, 10.2514/6.2023-1964.
- [28] P. R. Chai and A. W. Wilhite, "Cryogenic thermal system analysis for orbital propellant depot," *Acta Astronautica*, Vol. 102, Sep 2014, p. 35–46, 10.1016/j.actaastro.2014.05.013.
- [29] J. Borowsky, J. Charbonneau, J. Dougherty, A. Lagle, N. Masse, J. Mitchell, D. Patel, R. Veguilla, and J. Jayachandran, "Mitigating Boil-Off in Cryogenic Spacecraft Propellant Tanks," Mar 2023. Worcester Polytechnic Institute.
- [30] W. E. Hart, J.-P. Watson, and D. L. Woodruff, "Pyomo: modeling and solving mathematical programs in Python," *Mathematical Programming Computation*, Vol. 3, No. 3, 2011, pp. 219–260.
- [31] M. L. Bynum, G. A. Hackebeil, W. E. Hart, C. D. Laird, B. L. Nicholson, J. D. Sirola, J.-P. Watson, and D. L. Woodruff, *Pyomo—optimization modeling in python*, Vol. 67. Springer Science & Business Media, third ed., 2021.
- [32] Gurobi Optimization, LLC, "Gurobi Optimizer Reference Manual," 2022.
- [33] C. Warner, "First Commercial Moon Delivery Assignments to Advance Artemis," NASA, Jan 2020. Accessed: 2023-05-29.
- [34] B. Dunbar, "Commercial Lunar Payload Services Overview," NASA, Nov 2019. Accessed: 2022-11-18.
- [35] E. Vitug, "Polar Resources Ice Mining Experiment-1 (PRIME-1)," NASA, Jul 2020. Accessed: 2022-11-18.

- [36] A. Colaprete, “A lunar water reconnaissance mission,” *NASA*, 2020, p. 25. Accessed: 2022-11-18.
- [37] S. Potter, “NASA Selects Firefly Aerospace for Artemis Commercial Moon Delivery,” *NASA*, Feb 2021. Accessed: 2022-11-18.
- [38] G. Dodson, “NASA Selects Draper to Fly Research to Far Side of Moon,” *NASA*, Jul 2022. Accessed: 2022-11-18.
- [39] Astrobotic, “Astrobotic - Payload User Guide,” 2019. Accessed: 2022-11-18.
- [40] Aerojet Rocketdyne, “RL10 Propulsion System,” Apr 2022. Accessed: 2023-07-26.
- [41] Astrobotic, “Astrobotic Lunar Landers Payload User’s Guide v.5,” 2021. Accessed: 2022-11-18.
- [42] Astrobotic, “Griffin Lunar Test Model Complete,” Feb 2022. Accessed: 2022-11-18.
- [43] Blue Origin, “Blue Moon,” 2022. Accessed: 2022-11-16.
- [44] Blue Origin, “New Glenn Payload User’s Guide,” 2018.
- [45] ispace, “Payload User’s Guide,” 2020.
- [46] ispace, “ispace Unveils Mission 3 Lander Design, Set to Launch in 2024,” 2021. Accessed: 2022-11-18.
- [47] Firefly Aerospace, “Blue Ghost Lunar Lander Condensed Payload User’s Guide,” 2021.
- [48] E. Berger, “For lunar cargo delivery, NASA accepts risk in return for low prices,” *Ars Technica*, May 2021. Accessed: 2022-11-18.
- [49] Lockheed Martin, “McCandless Lunar Lander User’s Guide,” 2019. Accessed: 2022-11-18.
- [50] Moon Express, “MX-1 Scout Class Explorer,” Oct 2019. Accessed: 2022-11-01.
- [51] International Space Exploration Coordination Group (ISECG), “Global Exploration Roadmap (GER) Supplement August 2020: Lunar Surface Exploration Scenario Update,” 2020.
- [52] M. Landgraf, “Pathways to Sustainability in Lunar Exploration Architectures,” *Journal of Spacecraft and Rockets*, Vol. 58, Nov 2021, p. 1681–1693, 10.2514/1.A35019.
- [53] J. Guidi, M. Haese, M. Landgraf, C. Lange, S. Pirrotta, and N. Sato, “The 2022 Updated Lunar Exploration Scenario for the Global Exploration Roadmap (GER): The Growing Global Effort and Momentum Going Forward to the Moon and Mars,” *73rd International Astronautical Congress*, Paris, France, 2022.
- [54] M. Landgraf, L. Duvet, A. Cropp, G. Alvarez, G. Ambroszkiewicz, M. Bottacini, P. Brunner, L. Bucci, W. Carey, A. E. M. Casini, G. Cifani, O. Dubois-Matra, J. Ellwood, A. Gonzalez Fernandez, A. Ger-noth, A. Getimis, G. Gonzalez Gomez, D. Greuel, P. Hager, S. Heindel, M. Lanucara, Y. Le Deuff, S. Mangunsong, N. P. Murray, C.-V. Nardi, R. Nasca, K. Nergaard, G. Nzokira, F. Renk, D. Rovelli, J. Schlutz, R. Schonenborg, K. Stephenson, A. Tavoularis, N. Termtanasombat, A. Thirkettle, S. Ventura, B. S. d. l. Villa, M. Wohlhuter, and G. Magistrati, “Autonomous Access to the Moon for Europe: The European Large Logistic Lander,” *73rd International Astronautical Congress*, Paris, France, Sep 2022.
- [55] ArianeGroup, “Vinci Engine,” 2020. Accessed: 2023-07-28.